Available online at www.sciencedirect.com
SCIENCE DIRECT
ELSEVIER
International Journal of Mass Spectrometry 249–250 (2006) 330–339
International Journal of Mass Spectrometry
www.elsevier.com/locate/ijms

Analysis of kinetic energy release distributions by the maximum entropy method

B. Leyh *, E. Gridelet, R. Locht, J.C. Lorquet

Department of Chemistry, Molecular Dynamics Laboratory, Building B6c, University of Liège, B-4000 SART-TILMAN, Belgium

Received 19 October 2005; received in revised form 29 November 2005; accepted 7 December 2005
Available online 20 January 2006

Abstract

Energy is not always fully randomized in an activated molecule because of the existence of dynamical constraints. An analysis of kinetic energy release distributions (KERDs) of dissociation fragments by the maximum entropy method (MEM) provides information on the efficiency of the energy flow between the reaction coordinate and the remaining degrees of freedom during the fragmentation. For example, for barrierless cleavages, large translational energy releases are disfavoured while energy channeling into the rotational and vibrational degrees of freedom of the pair of fragments is increased with respect to a purely statistical partitioning. Hydrogen atom loss reactions provide an exception to this propensity rule. An ergodicity index, F, can be derived. It represents an upper bound to the ratio between two volumes of phase space: that effectively explored during the reaction and that in principle available at the internal energy E. The function $F(E)$ has been found to initially decrease and to level off at high internal energies.

For an atom loss reaction, the orbiting transition state version of phase space theory (OTST) is especially valid for low internal energies, low total angular momentum, large reduced mass of the pair of fragments, large rotational constant of the fragment ion, and large polarizability of the released atom. For barrierless dissociations, the major constraint that results from conservation of angular momentum is a propensity to confine the translational motion to a two-dimensional space. For high rotational quantum numbers, the influence of conservation of angular momentum cannot be separated from effects resulting from the curvature of the reaction path.

The nonlinear relationship between the average translational energy $\langle\varepsilon\rangle$ and the internal energy E is determined by the density of vibrational–rotational states of the pair of fragments and also by non-statistical effects related to the incompleteness of phase space exploration.

The MEM analysis of experimental KERDs suggests that many simple reactions can be described by the reaction path Hamiltonian (RPH) model and provides a criterion for the validity of this method.

Chemically oriented problems can also be solved by this approach. A few examples are discussed: determination of branching ratios between competitive channels, reactions involving a reverse activation barrier, nonadiabatic mechanisms, and isolated state decay.

Keywords: Angular momentum; Ergodicity; Maximum entropy; Translational energy release; Nonadiabatic reactions

1. Statistical methods in mass spectrometry

For the last 50 years, mass spectrometrists have made great efforts to rationalize fragmentation patterns and breakdown graphs by various statistical models that are all based on a common assumption. The internal energy deposited in a molecular ion is expected to be completely randomized before dissociation [1–4]. When this is the case, the reaction is declared ergodic. Equivalently, the energetically available phase space is said to be uniformly sampled within the lifetime of the molecular ion. In still more esoteric terms, the molecular ion is said to have reached a state of microcanonical equilibrium, or to be close to it; hence the denomination "quasi-equilibrium theory" (QET) adopted by Rosenstock and coworkers [4].

However, full energy randomization in an activated molecule can be prevented by dynamical constraints. The conservation of total angular momentum has often been invoked, but less obvious conservation laws or propensities might exist. In fact, it has been argued [5] that phase space can never be ergodically explored prior to dissociation in a unimolecular reaction. For-

* Corresponding author. Tel.: +32 4 3663425; fax: +32 4 3663413.
E-mail address: Bernard.Leyh@ulg.ac.be (B. Leyh).

1387-3806/$ – see front matter © 2005 Elsevier B.V. All rights reserved.
doi:10.1016/j.ijms.2005.12.005

tunately, this is not necessary. Statistical models will work in spite of the existence of dynamical constraints if phase space is representatively sampled.

2. Of the importance of studying KERDs

To what extent is this ergodic assumption supported by experimental data on ionic unimolecular dissociations?

To discuss criterions for non-ergodicity, it is essential to distinguish between the study of the rate constants and that of the product energy distributions. The study of kinetic energy release distributions (KERDs) offers considerable advantages. As shown by many authors, with Chava Lifshitz at the forefront [1,6–12], KERDs are more sensitive than rate constants to deviations from statistical expectations. The reason is easily seen.

Let us denote as $P(\varepsilon|E)$ the probability of generating fragments with a relative translational energy equal to ε if E is the internal energy, measured in excess of the dissociation threshold. Then,

$$P(\varepsilon|E) = \frac{k_{\mathrm{diss}}(E,\varepsilon)}{\int_0^E k_{\mathrm{diss}}(E,\varepsilon)\,\mathrm{d}\varepsilon} = \frac{k_{\mathrm{diss}}(E,\varepsilon)}{k_{\mathrm{diss}}(E)} \tag{1}$$

where $k_{\mathrm{diss}}(E,\ \varepsilon)$ denotes the detailed translational-energy resolved rate constant (expressed in units energy^{-1} time^{-1}). By contrast, the usual rate constant $k_{\mathrm{diss}}(E)$ (expressed in units time^{-1}) provides an integrated (and thus less sensitive) information.

The dichotomy between the observables $k_{\mathrm{diss}}(E)$ and $P(\varepsilon|E)$ is paralleled by another one, which concerns the two well-established statistical theories of unimolecular reactions with which mass spectrometrists are familiar. The first one is the Rice–Ramsperger–Kassel–Marcus (RRKM) theory [1–3], which is practically identical with QET [4]. The second one, first proposed by Klots [13,14] but mainly developed by Chesnavich and Bowers in an impressive series of papers [15–19], is a variant of phase space theory that studies reactions involving very loose orbiting transition states (OTS). It is hereafter denoted OTST [1,3,10,15–22]. Each theory is particularly adapted to a specific type of experiment.

The RRKM–QET theory predicts the variation of the unimolecular rate constant with internal energy. Since a transition-state calculation requires consideration of the properties of the system at short values of the reaction coordinate, i.e., up to the transition state only, it assumes short-range forces and strong intermode couplings. By contrast, OTST is especially suited for calculating KERDs. It focusses on long-range weak interactions between separating fragments at asymptotic values of the reaction coordinate. The angular momentum of each fragment as well as that generated by their relative motion, termed the orbital motion, play a leading role in the formulation of these interactions. Let us now review the basic assumptions of OTST and discuss briefly their validity domain.

3. OTST

3.1. Basic assumptions

Ionic systems are characterized by a long-range interaction potential. Therefore, a central-field assumption describing the interaction between a point charge and an induced dipole can be expected to provide a reasonable starting point for barrierless unimolecular reactions (i.e., when no reverse activation barrier is encountered along the reaction path). The location of the centrifugal barrier depends on the value of the orbital angular momentum. Several assumptions and limitations have to be introduced to make the model tractable.

Let us restrict to the particularly simple case of reactions where the fragments can be modelled as a spherical or linear top carrying a positive charge interacting with a polarizable atom. The argument proceeds as follows [1,3,10,15–22].

(1) An effective potential $V_{\mathrm{eff}}(r)$ is generated by adding a quasidiatomic centrifugal term and a rotational term to the spherically symmetric potential that characterizes the charge-induced dipole interaction:

$$V_{\mathrm{eff}}(r) = -\frac{\alpha q^2}{2r^4} + \frac{\ell^2\overline{h}^2}{2\mu r^2} + Bj^2 \tag{2}$$

where α is the polarizability of the noncharged partner, q the ionic charge, μ the reduced mass of the fragments, ℓ the quantum number of their orbital motion, B the rotational constant of the charged fragment and j is its quantum number. The effective potential $V_{\mathrm{eff}}(r)$ has its maximum when the fragments are separated by a distance r_{c} equal to

$$r_{\mathrm{c}} = \frac{(2\mu\alpha q^2)^{1/2}}{\ell\overline{h}} \tag{3}$$

The KERD can be expected to be reliably calculated only if the distance r_{c} is large enough to be located in a region where Eq. (2) is valid, i.e., where the assumption of an isotropic ion-induced dipole potential is reliable. Eq. (3) shows that large values of ℓ are a cause for concern.

The orbiting energy at the transition state

$$V_{\mathrm{eff}}(r_{\mathrm{c}},\ \ell) - Bj^2 = \frac{\ell^4\overline{h}^4}{8\mu^2\alpha q^2} \tag{4}$$

is assumed to be adiabatically converted into fragment translational energy.

(2) OTST is based on the principle of microscopic reversibility (also termed detailed balance theorem) [1–3,20–22], which establishes a relationship between the unimolecular translational energy-resolved dissociation rate constant $k_{\mathrm{diss}}(E,\ \varepsilon)$ and the rate constant of the recombination reaction k_{rec}, which is proportional to the capture cross section σ_{capt}.

(3) An expression for σ_{capt} can be formulated provided that the total angular momentum $J\overline{h}$ (which is strictly conserved) is, in the entire region extending from the maximum of V_{eff} to an infinite distance between the fragments, expressible as the vectorial sum of two individual momenta, $j\overline{h}$ (rotational

angular momentum of the neutral fragment), and $\ell\overline{h}$ (angular momentum deriving from the orbital motion of the pair of fragments). This can only be true if the centrifugal barrier r_c occurs at very large interfragment separations so that both ℓ and j may be assumed to remain good quantum numbers in the range $[r_c, +\infty]$.

The fragments are captured (or the fragmentation takes place) if two conditions are fulfilled:

(a) The angular momentum must be conserved, i.e.,

$$|J - j| \leq \ell \leq J + j \tag{5}$$

and

(b) the translational energy must be high enough to overcome the centrifugal barrier:

$$\varepsilon \geq V_{\text{eff}}(r_c, \ell) - Bj^2 \tag{6}$$

Furthermore, it can be demonstrated [22] that the previous equations lead to an $\varepsilon^{1/2}$ threshold law for the J-resolved KERD, $P_{\text{OTST}}(\varepsilon|E, J)$

$$\lim_{\varepsilon\to 0} P_{\text{OTST}}(\varepsilon|E, J) \propto \varepsilon^{1/2} \tag{7}$$

3.2. Range of validity

A detailed study of the conditions of validity of OTST applied to ionic dissociations has been recently carried out [22]. It agrees with other investigations on neutral fragmentations [23]. In qualitative terms, the conclusions can be summarized as follows. OTST loses progressively its validity when the internal energy E and the total angular momentum J increase, and when the reduced mass μ, the rotational constant B of the molecular fragment, and the polarizability α of the released atom decrease.

A more detailed appraisal has been made in the particular case of fragmentations leading to a phenyl cation plus an atom studied in the metastable time window of a sector mass spectrometer [22]. OTST is quantitatively reliable for the dissociation of the iodobenzene ion only, provided that the reaction is studied at internal energies as low as possible, i.e., preferably in the second field-free region of a reverse geometry instrument. The theory is of qualitative value only for reactions leading to the release of a bromine or chlorine atom and is no longer valid when a hydrogen atom is released. At higher internal energies, the constraints resulting from the conservation of angular momentum have been shown [24,25] to be inextricably intermingled with those resulting from the curvature of the reaction path. This point will be more fully developed in Section 5.2.

For these reasons, the conclusions reached by Lim et al. [26] who apply phase space theory to the dissociation of the bromobenzene ion on a nanosecond time scale, sometimes considering internal energies as high as 10 eV seem to us questionable. The inadequacy of OTST at too high energies may explain why this theory is unable to provide an adequate fit to the experimental data unless the critical energy of the reaction is taken as an adjustable parameter.

4. Maximum entropy method

4.1. General presentation

The purpose of the present review is to discuss an alternative strategy, in addition to predictive theories like RRKM and OTST. It will be shown that the maximum entropy method (MEM) makes it possible to identify the presence of dynamical constraints from an analysis of experimental KERDs [27–31]. Chava Lifshitz was the first to recognize the power of the newly developed method [7]. The strengths of the MEM approach can be summarized as follows.

(1) As noted, e.g., by Forst [32], transition state theory uses the methods of equilibrium statistical mechanics in what is basically a nonequilibrium situation. (Hence, the "quasi-" restriction in QET.) The same remark applies to OTST because of its use of the principle of microscopic reversibility. By contrast, MEM remains valid for nonequilibrium situations [27–31]. It is free from the shortcoming that constantly worried Rosenstock [4] when he was expounding his quasi-equilibrium assumption: "The extent of nonequilibrium is debatable . . . It must be emphasized that the use of the microcanonical ensemble is not secure". Furthermore, the method is very general: unlike OTST, its validity is not restricted to a given internal energy range.

(2) The essence of MEM is to upgrade a statistical reference theory by a stepwise procedure. The improvement can in principle, but not in practice, be carried out up to an exact solution of the Schrödinger equation [28]. In practice, it only makes sense to improve the solution up to a point where the difference between experiment and theory is of the same magnitude as the experimental uncertainty. MEM can also be viewed as an interpolation between the RRKM model (characterized by free energy flow among all modes, without any constraint) and the Slater model (which is highly constrained because the assumed harmonic nature of the vibrations prevents any energy exchange) [30].

(3) Note especially that the origin of the maximum entropy method is the desire to derive the least biased inference from a given situation. Its very aim is precisely to avoid pushing the data analysis too far. It can be credited with impressive success in the analysis of product energy distributions observed in the dissociation of neutral molecules [28–31].

(4) The MEM explains the origin of the success of the RRKM theory. According to information theory, when phase space is not completely or not uniformly sampled before dissociation, the statistical theory should be developed in terms of effective densities of states, which count an effective number of phase space cells. These new densities, invariably, have a lower value than those that are calculated by usual state-counting algorithms [1–3]. This more elaborate formulation replaces the concept of "effective number of oscillators" widely used in the past. This is compatible, e.g., with the Local Random Matrix Theory approach which upgrades the RRKM theory by introducing a transmission coefficient accounting for the competition between the intrinsic reac-

tion rate and the intramolecular energy flow. The latter is shown to vary with the local density of vibrational states which is necessarily smaller than the total reactant density of states [33,34].

It is worth noting that the density of states lowering applies in principle, but not of course necessarily to the same extent, to both the reactant and the transition state. Hence, the RRKM equation

$$k(E) = \frac{N^{\ddagger}(E - E_0)}{h\rho(E)} \tag{8}$$

remains valid, but both its numerator and denominator should be reduced. In other words, the deviations from RRKM are not so strong as might be expected [35,36]. For this reason, the RRKM–QET formula is not so sensitive to moderate non-statistical effects. Its success does not unambiguously prove that its basic assumptions are valid. By contrast, a KERD is more sensitive to any deviation from the statistical situation than the rate constant because this compensation mechanism does not operate for the KERD.

(5) It is essential to note the unusual viewpoint and strategy of the MEM. Unlike OTST, its aim is not to predict quantitatively a KERD, but rather to analyze experimental data in order to assess the efficiency of phase space sampling and to identify the dynamical constraints that prevent ergodicity. MEM has thus to be considered as a complementary approach rather than as a competitor to predictive theories. How MEM works in practice is developed in the next sections.

4.2. The prior distribution

The maximum entropy method starts by considering a fully statistical situation where all quantum states of the pair of fragments which are allowed by energy conservation are populated with the same probability. The corresponding distribution of translational energies is called the prior distribution [1,27–31] and is denoted as $P^0(\varepsilon|E)$. By its very definition, it is proportional to the total density of states. At a given total energy E (measured with respect to the dissociation threshold), if ε is the amount of energy that has flowed into the reaction coordinate, then the remainder $(E - \varepsilon)$ is deposited in the fragments. Denoting as $\rho_{vr}(E - \varepsilon)$ the density of vibrational–rotational states of the pair of fragments, one has simply

$$P^0(\varepsilon|E) \propto \varepsilon^{1/2}\rho_{vr}(E - \varepsilon) \tag{9}$$

because the density of translational states in a three-dimensional space distribution [1,27–31] is proportional to $\varepsilon^{1/2}$.

Note that the constraint resulting from conservation of angular momentum is completely disregarded in the definition of the prior distribution, for the very simple reason that no exact treatment about it is available. It should be carefully kept in mind that the prior distribution represents, in the MEM procedure, a reference and not a crude and mediocre first approximation to the exact KERD. Its aim is to provide a criterion of non-ergodicity: if the experimental distribution $P(\varepsilon|E)$ differs from $P^0(\varepsilon|E)$, then it can be concluded that one or several dynamical constraints introduce a bias in the exploration of phase space, favouring some quantum states at the expense of others. These constraints are possibly related to angular momentum conservation, but other possibilities cannot be a priori excluded.

4.3. MEM expression of the actual KERDs

When the experimental KERD $P(\varepsilon|E)$ is found to differ from the prior distribution $P^0(\varepsilon|E)$, the MEM establishes that the least biased way to convert the latter into the former is to multiply it by a correcting exponential function of ε.

$$P(\varepsilon|E) = P^0(\varepsilon|E)\exp(-\lambda_0)\exp(-\lambda_1\varepsilon^k) \tag{10}$$

In this equation, the quantity λ_1 is a Lagrange multiplier in a process that consists in making the dissociation dynamics as statistical as allowed by the constraint. The factor $\exp(-\lambda_0)$ is simply a normalization factor determined by the condition that the distributions $P(\varepsilon|E)$ and $P^0(\varepsilon|E)$ should both be normalized in the following way:

$$\int_0^E P(\varepsilon|E)\,\mathrm{d}\varepsilon = \int_0^E P^0(\varepsilon|E)\,\mathrm{d}\varepsilon = 1 \tag{11}$$

In many cases [22,37–44], the very simple expression (10) is found to provide a very good approximation to $P(\varepsilon|E)$ if the value of the exponent k is adequately chosen. A value of k equal to 1/2 or to 1 is usually found. For electronically adiabatic barrierless reactions studied at not too high energies, the appropriate value of k has been observed to be equal to 1/2 [22,37–41,43,44]. Then, the actual KERD is related to the prior distribution by the following equation:

$$P(\varepsilon|E) = \mathrm{e}^{-\lambda_0}\,\mathrm{e}^{-\lambda_1\varepsilon^{1/2}}P^0(\varepsilon|E) \tag{12}$$

where the only unknown is λ_1.

In such a case, the unimolecular distribution of ions is subject to a dynamical constraint that is directly related to the square root of the translational energy ε, i.e., to the linear momentum of the separating fragments. Its physical meaning will be elaborated upon in Section 5.2.

In principle, the prior distribution should be submitted to a sequence of multiplicative corrections

$$P(\varepsilon|E) = P^0(\varepsilon|E)\exp(-\lambda_0)\exp(-\lambda_1\varepsilon^{1/2})\exp(-\lambda_2\varepsilon) \times \exp(-\lambda_3\varepsilon^2)\ldots \tag{13}$$

It has been demonstrated [28] that if the number of factors $\exp[-\lambda_i\varepsilon^{ki}]$ is large enough, then the right-hand side of Eq. (13) converges to an exact quantum-mechanical result for $P(\varepsilon|E)$. However, the practical feature that makes the MEM interesting is that only a very small number of dynamical constraints (usually, just one for barrierless reactions) are needed to transform the prior distribution into a shape very close to the experimentally observed distribution. For more complicated chemical processes, two or three factors may be required [43,44].

4.4. Entropy S and entropy deficiency DS

It is possible to characterize a KERD by its entropy S, which is directly linked to the number of configurations that give rise to this particular distribution, as shown by Boltzmann's equation for the prior distribution $S_0 = \ln W$. (In information theory, entropies are dimensionless, i.e., Boltzmann's constant is set equal to 1.) Hence, the prior distribution P^0, which is the most statistical one, has the highest possible entropy S_0. The presence of dynamical constraints leads to incomplete phase space sampling and reduces the entropy S. The exponential relation $W = \exp(S)$ between an effective number of states W and an entropy S also applies when phase space is not uniformly or not completely sampled.

The difference between the entropies of the prior distribution $P^0(\varepsilon|E)$ and of an experimental KERD $P(\varepsilon|E)$ is termed the entropy deficiency DS, which is defined as [27–31]:

$$\mathrm{DS} = S_0 - S = \int_0^E P(\varepsilon\,|E)\ln\left[\frac{P(\varepsilon|E)}{P^0(\varepsilon|E)}\right]\mathrm{d}\varepsilon = -\lambda_0 - \lambda_1\langle\varepsilon^k\rangle \geq 0 \quad (14)$$

where $\langle\varepsilon^k\rangle$ denotes the kth order moment of the distribution:

$$\langle\varepsilon^k\rangle = \int_0^E \varepsilon^k P(\varepsilon|E)\,\mathrm{d}\varepsilon \quad (15)$$

A nonzero value for DS implies that the pair of fragments does not explore the whole of the phase space that is compatible with the mere specification of the internal energy.

4.5. Ergodicity index F

A major interest of the concept of entropy deficiency is that it can be used to derive an ergodicity index. It can be demonstrated [45,46] that the quantity

$$F \equiv \exp(-\mathrm{DS}) = \exp(\lambda_0 + \lambda_1\langle\varepsilon^{1/2}\rangle + \ldots) \quad (16)$$

is an upper bound to the ratio between two volumes of phase space: that actually explored by the dissociating system and that in principle available at the total energy E.

A value of $F = 1$ indicates that the energy flow between the reaction coordinate and the bath of the remaining vibrotational degrees of freedom is completely unhindered.

It should be realized that the index F derived from KERD data measures only the coupling between the reaction coordinate and the bath formed by the remaining oscillators. Therefore, it provides an upper limit to a real ergodicity index because restrictions to phase space exploration that do not affect the kinetic energy release (e.g., the energy exchange among oscillators) are not taken into account in its definition.

4.6. Energy dependence

In addition to techniques like MIKES (mass-analyzed ion kinetic energy spectrometry), which analyze the KERD on the microsecond time scale, two experimental approaches are available to measure KERDs at higher values of the internal energy E: PEPICO [11,47], and retarding field methods [21,40,42,44]. The KERD measured with the MIKES and retarding field techniques is actually an average over an internal energy distribution $D(E)$: it will be denoted as $\tilde{P}(\varepsilon)$.

In a MIKES experiment, the Lagrange parameters can be assumed to remain constant in the narrow metastable range. Hence, $\tilde{P}(\varepsilon)$ is given by:

$$\tilde{P}(\varepsilon) = \int_\varepsilon^\infty D(E)P(\varepsilon\,|E)\,\mathrm{d}E = \int_\varepsilon^\infty D(E)P^0(\varepsilon\,|E)\ \exp[-\lambda_0 - \lambda_1\,\varepsilon^k]\,\mathrm{d}E \quad (17)$$

with $D(E) = \exp[-k_{\mathrm{diss}}(E)\tau_1] - \exp[-k_{\mathrm{diss}}(E)\tau_2]$, where τ_1 and τ_2 denote the entry and exit times in the field-free region.

In a PEPICO experiment, the distribution $D(E)$ is a very narrow bell-shaped function and Eqs. (10), (12), or (13) are directly usable.

In a retarding field experiment, the experimental set-up is characterized by a wide (a few eV) distribution of internal energies, $D(E)$, that is given by the product of the photoelectron spectrum of the parent molecule and of the branching ratio of the selected dissociation channel. Therefore, the KERD is again expressed by Eq. (17) with energy-dependent Lagrange parameters.

When the Lagrange multipliers derived from Eq. (17) are introduced into Eq. (16), a function $F(E)$ can be derived, which expresses the way the efficiency of phase space exploration varies with the internal energy of the molecular ion [40,42,48]. The results will be discussed in Section 5.4.

5. Analysis of the experimental results

5.1. General propensities

Let us first analyze the simplest possible reactions, i.e., those that

(i) are electronically adiabatic (no curve-crossing, no excited state involved in the mechanism);
(ii) proceed without any reverse potential energy barrier;
(iii) are studied at the lowest amount of internal energy, i.e., often as a metastable fragmentation.

Chava Lifshitz [49–51] singled out the halogen loss reaction of bromo- and iodobenzene as particularly simple. The HCN loss from the pyridine cation can be joined to them [39].

The KERD of these reactions is found to obey Eq. (17) remarkably well (Fig. 1). Thus, only a single constraint, to be identified with the linear momentum resulting from the relative translational motion of the separating fragments can be detected. Furthermore, the Lagrange multiplier λ_1 is found to be positive, which implies that less translational energy flows into the reaction coordinate than the statistical estimate. The index F is of the order of 75–80%. What is the missing percentage due to? Is it related to angular momentum conservation?

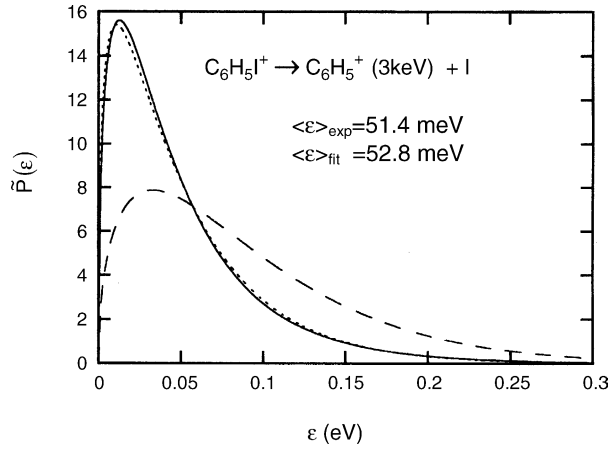

Fig. 1. KERD for the iodine loss reaction from the iodobenzene cation taking place in the first field-free region of a forward geometry two sector mass spectrometer [38]. The translational energy of the ionic fragment in the laboratory reference frame is set at 3 keV. Solid line: experimental distribution. Dotted line: fitted distribution using Eq. (17) with $k = 1/2$. Dashed line: prior distribution at $E = 0.62$ eV, corresponding to the most probable internal energy of the dissociating iodobenzene ion.

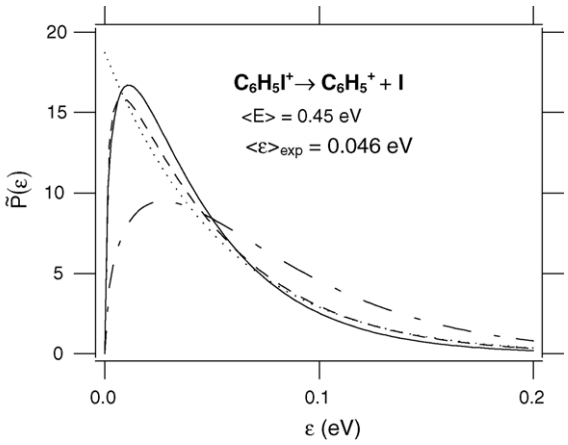

Fig. 2. KERD for the $C_6H_5I^+ \rightarrow C_6H_5^+ + I$ reaction taking place in the second field-free region of a forward geometry two sector mass spectrometer (translational energy in the laboratory frame: 8 keV). Solid line: experiment. Dashes: OTST calculation. Dots: two-dimensional prior distribution. Dot-dashes: three-dimensional prior distribution.

To get a deeper insight, let us first consider a particularly simple reaction, i.e., the dissociation of the iodobenzene cation studied at a low internal energy (i.e., ≈0.45 eV above the dissociation asymptote). In that case, OTST is quantitatively valid [22]. Then, conservation of angular momentum constrains the nuclear trajectories to be planar because ℓ remains a good quantum number. This well-known constraint can be included in the prior distribution to be used in an alternative MEM analysis. Since the density of translational states of a particle moving in a two-dimensional box is a constant [1], the appropriate prior distribution is simply proportional to $\rho_{vr}(E-\varepsilon)$, and thus is a steadily decreasing function of ε. It will be denoted as $P^0_{2D}(\varepsilon|E)$:

$$P^0_{2D}(\varepsilon\,|E\,) \propto \rho_{vr}(E-\varepsilon) \tag{18}$$

and should be compared with Eq. (9).

Fig. 2 shows that this two-dimensional prior distribution provides a good approximation to the actual KERD of the iodobenzene cation measured at a low internal energy E. The agreement is much better than with the three-dimensional prior $P(\varepsilon|E)$ given by Eq. (9). In other words, the major constraint that affects the experimental KERD is the requirement that the translational motion be two-dimensional.

However, an additional constraint is clearly seen to operate on $P^0_{2D}(\varepsilon|E)$. It is responsible for the threshold behaviour of the KERD and takes the form of a truncation resulting from the requirement that the translational energy be large enough to surmount the orbital barrier.

We now turn to not so straightforward situations. At higher internal energies or when an atom less massive or less polarizable than iodine is released, the OTST assumptions become unreliable. The dynamics then takes place in a range of internuclear distances where the effective potential energy can no longer be assumed to be spherically symmetrical and therefore no longer obeys Eq. (2). A more realistic interaction potential should include higher-order terms in its multipolar expansion, and would be contaminated by anisotropic short-range valence contributions.

This situation is encountered in the study of the KERD of bromobenzene or of iodobenzene measured at a higher internal energy (i.e., ≈0.6–0.8 eV above the dissociation asymptote). In such a case: (i) OTST becomes invalid [22,23]; (ii) the MEM equation (12), with a three-dimensional prior and a $\varepsilon^{1/2}$ constraint still gives an excellent description of the experimental results; (iii) the use of a 2D prior loses its appeal but still hints that the confinement to a two-dimensional space subsists as a propensity. This surprising conclusion is a matter of current research.

5.2. Interpretation of the momentum constraint

OTST fails at high internal energies because ℓ and j are then no longer good quantum numbers in the whole reaction coordinate range from the centrifugal barrier outwards. An alternative model that can manage this situation has been proposed by Miller and coworkers.

The basis of the reaction path Hamiltonian (RPH) model [24,25,52] is to consider only the potential energy surface in the immediate neighbourhood of the reaction coordinate. If the internal energy is not too high, the dynamical motion can be expected not to deviate too far from the minimum energy path, at least in a certain range. The motion along the reaction path can then be described as a translation, with the modes orthogonal to it treated as molecular vibrations. If so, the region of the potential energy surface that influences the dynamics can be modelled as a $(3N-7)$-dimensional harmonic valley about the reaction coordinate. Energy transfer among these degrees of freedom results mainly from the curvature of the reaction path. However, Miller and coworkers could derive a coupling parameter [24]. When the latter is small enough, the reaction coordinate is decoupled from the bath of oscillators and the dynamics can be described as a one-dimensional motion in an effective potential. Moreover, recent research [53] has shown that when the RPH

model is valid in a particular range of the reaction coordinate, the dynamical constraint bears automatically on the momentum, i.e., on $\varepsilon^{1/2}$. Then, the KERD is expressed by the very simple MEM Eq. (12) with λ_1 positive. Finally, Miller et al. could show [24] that when the total angular momentum J is large, it strongly interacts with the coupling that results from the curvature. As a consequence, it is no longer possible to sort out the constraints related to angular momentum conservation and those resulting from the curvature of the reaction path.

Conversely, experimental evidence that the constraint is equal to $\varepsilon^{1/2}$ can be interpreted as a suggestion that the last step of the reaction should be studied by the RPH model.

5.3. Average translational energy release

Average translational energy releases $\langle\varepsilon\rangle$ are defined by

$$\langle\varepsilon\rangle = \int_0^E \varepsilon P(\varepsilon|E)\,\mathrm{d}\varepsilon \tag{19}$$

Let us again restrict the discussion to simple (i.e., electronically adiabatic, barrierless) reactions, for which the constraint is the linear momentum $\varepsilon^{1/2}$. The KERD is then given by Eq. (12), with energy-dependent Lagrange parameters. It follows from Eqs. (10) and (12) that when the Lagrange multiplier λ_1 is positive the released translational energy is less than what is predicted by the prior distribution, i.e., is less than what is expected from a fully statistical theory.

A MEM analysis reveals that the average kinetic energy release $\langle\varepsilon\rangle$ does not necessarily increase linearly with the internal energy E [48]. In fact, it is determined by two quantities. First, the logarithmic derivative of $\rho_{vr}(E)$, i.e., its slope when plotted on a logarithmic scale. Second, the ratio $\langle\varepsilon\rangle/E$ also depends on non-statistical effects, i.e., on incomplete phase space exploration, which is measured by the energy-dependent entropy deficiency DS and the ergodicity index e^{-DS}. For these simple reactions, simple relationships can be derived from Eqs. (9), (12), and (16) to relate the value of $\langle\varepsilon\rangle/E$ to that of e^{-DS} and $\mathrm{d}\ln(\rho_{vr})/\mathrm{d}E$. Here again, the MEM replaces the vague concept of "subset of active degrees of freedom" used in the Haney–Franklin relationship [54] by that of "ergodicity index measuring the extent of phase space sampling".

5.4. Efficiency of phase space sampling as a function of the internal energy

A very interesting question concerns the energy-dependence of the ergodicity index

$$F(E) = \exp[-\mathrm{DS}(E)] = \exp[\lambda_0(E) + \lambda_1(E)\langle\varepsilon^{1/2}\rangle(E) + \ldots] \tag{20}$$

At threshold ($E = 0$), $F = 1$ because the phase space reduces to a single cell. The system necessarily occupies 100% of its available phase space when there is no other choice. An increase of E leads to the metastable window with F values typically observed in the 75–80% range. At still higher internal energies, F keeps on decreasing but is found to level off or even re-increase, say at $E \approx 2.5$ eV, where it reaches its lowest value, which is roughly of the order of 50% for the investigated reactions. This behaviour has been observed in a number of cases: loss of a Br atom from $C_2H_3Br^+$ [40], loss of I from $C_2H_5I^+$ [48], HCN loss from the pyridine ion [42] and, very recently, loss of an acetylene molecule from $C_6H_6^+$ ions.[1]

As the internal energy increases, the lifetime decreases whereas the volume of phase space to be sampled increases enormously. The molecule has less time to sample a greater volume of phase space before dissociating. The initial decrease of the ergodicity index is thus quite understandable. What is surprising, however, is the stabilization or increase of $F(E)$ at higher internal energies.

Deciphering the mechanism responsible for this paradox clearly requires further work. We may, however, already note that intramolecular energy flow among oscillators resulting from the anharmonic character of the potential energy surface of the molecular ion in its ground electronic state is not the only mechanism by which energy gets redistributed. Very fast radiationless transitions that result from the numerous crossings among potential energy surfaces also contribute to energy randomization [40,42,55,56]. The higher the internal energy E, the more extended and intricate the pattern of surface crossings. This relaxation of the electronic energy via a cascade of non-radiative transitions leads to a great diversity of initial conditions and introduces chaos into the nuclear dynamics, as conjectured by Rosenstock 40 years ago [4]. Each point on the crossing seams is a possible origin of a reactive trajectory.

It follows that for most conventional ionization methods (i.e., electron impact, photoionization or chemical ionization), the initial conditions are scattered all over the phase space, just as for thermal reactions. The preparation is said to be non-specific. Therefore, a short lifetime deriving from a high internal energy does not necessarily preclude an efficient and representative phase space sampling.

5.5. Isomerization reactions

The MEM approach can also be used to derive chemical information, e.g., on the competition between reaction pathways leading to isomeric ions. Two examples have been investigated in detail: (i) the benzylium versus tropylium ion formation by hydrogen loss from the toluene cation and (ii) the competition between the cyclic and linear forms of $C_6H_5^+$ ions generated from protonated fluorobenzene.

The competition between isomeric tropylium and benzylium ion ($C_7H_7^+$) formation from the toluene cation ($C_7H_8^+$) has been investigated for many years by various techniques and the question has been reviewed by Chava Lifshitz in 1994 [57]. Based on the analysis of rate constant data, the tropylium/benzylium branching ratio could be determined as a function of the internal energy of $C_7H_8^+$. In the metastable time window, this ratio amounts to about one. Kim and coworkers [58] attempted in 2000 to derive the same ratio from KERD measurements, also

[1] E. Gridelet, A.J. Lorquet, J.C. Lorquet, R. Locht, B. Leyh, unpublished.

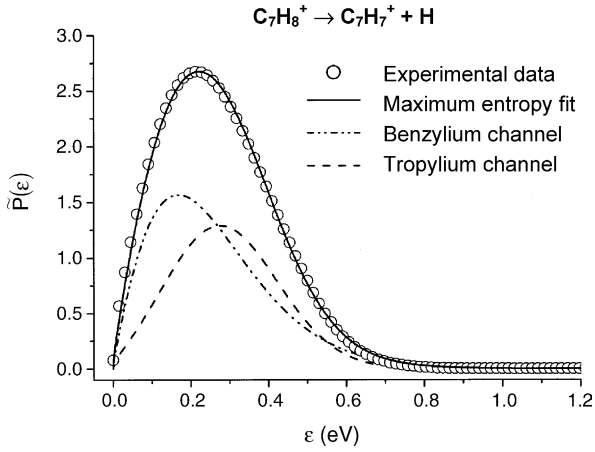

Fig. 3. KERD for the hydrogen loss from the toluene cation taking place in the first field-free region of a forward geometry two sector mass spectrometer. Fragment ion translational energy in the laboratory frame equal to 3 keV. Open circles: experiment. Solid line: fit using the maximum entropy method. Dashed-dotted line: contribution of the benzylium channel. Dashed line: contribution of the tropylium channel.

in the metastable range. The experimental H-loss KERD is composite and can be expressed as the sum of two contributions associated respectively with the tropylium and with the benzylium fragments (Fig. 3). These authors used the OTST formalism to modelize the benzylium production channel and deduced a 5:1 tropylium versus benzylium ratio, in complete disagreement with the previous data.

The maximum entropy formalism has been able to reconcile the KERD data with the rate constants [43]. The benzylium contribution could be fitted using a single constraint equal to $\varepsilon^{1/2}$. The associated Lagrange multiplier is, however, negative, indicating that more kinetic energy is released on the fragments than expected on statistical grounds and also more than predicted by OTST. The fraction of phase space sampled is found to be equal to $48 \pm 8\%$, i.e., far away from the statistical limit. It has been suggested that rotational energy flows preferentially in the reaction coordinate as a result of the conservation of a cylindrical symmetry axis during the fragmentation. For the tropylium channel, which involves a reverse activation barrier (see a more detailed discussion of that point in Section 5.6), two constraints are identified: ε and ε^2. The ergodicity index is in the 50–70% range, depending on the internal energy. This analysis allowed us to deduce a tropylium versus benzylium isomeric fraction equal to 0.9 ± 0.3 in the metastable window, in good agreement with experimental values obtained using photodissociation and charge exchange, and with RRKM calculations [57]. The origin of the discrepancy with Kim's result is clearly the inadequacy of the OTST formalism for hydrogen loss reactions. By contrast, the introduction of an appropriate constraint allows a much better description of the benzylium channel contribution and thus a more accurate determination of the branching ratio.

A second example concerns the competition for the production of cyclic and linear isomers of $C_6H_5^+$ during the fragmentation of protonated fluorobenzene. This time, the MEM analysis [41] confirms the interpretation originally proposed by Schröder et al. [59]. The KERD measured by these authors was found to be composite with a broad and intense component resulting from the generation of cyclic phenyl ions and a weak, low-kinetic energy component assigned to the production of one (or several) open-chain isomers of $C_6H_5^+$. The reactive fluxes were estimated by the MEM to be roughly in the ratio 16:1 for $C_6H_5F.H^+$ and 34:1 for $C_6D_5F.D^+$, in qualitative agreement with the (possibly more accurate) estimate of 10:1 and 18:1 obtained by Schröder et al.

5.6. Reverse activation barriers

Non-statistical behaviour is often observed when a reverse activation barrier, with a height E_b, plays a leading role in the dissociation. In this kind of reaction, denoted type II by Laskin and Lifshitz [10], the distribution is displaced to larger kinetic energies compared to the statistical expectation and its shape tends to be more Gaussian-like. To analyze the KERD, it is generally assumed that the observed translational energy has a double origin. The first component results from the partial conversion of the energy barrier, E_b, into translational energy. The second part comes from the so-called non-fixed internal energy in excess of the barrier, $E - E_b$. The average kinetic energy release can then be expressed as

$$\langle \varepsilon \rangle = a(E - E_b) + bE_b \tag{21}$$

where a and b are efficiency coefficients.

The energy partitioning of the non-fixed contribution tends to behave as in barrierless reactions. The conversion of the barrier, however, presents a highly non-statistical behaviour: about one-half of the energy of the barrier is released as translation with the other half released as rotation (or, less probably, vibration) of the fragments as a result of exit-channel interactions between receding fragments.

As an example, the reaction forming tropylium fragments by hydrogen loss from the toluene cation will be mentioned (Fig. 3) [43]. It has already been referred to in the previous subsection. This reaction involves an isomerization of the toluene cation to the cycloheptatriene structure followed by hydrogen loss leading to the tropylium ion. A reverse activation barrier of 0.43 eV has been calculated for this latter step [57]. The MEM analysis reveals that $41 \pm 7\%$ of this barrier is released as translation. The same result is obtained, within experimental errors, for the perdeuterated isomer. By contrast, only 5.5% of the non-fixed energy is converted into relative translation. For perdeuterated toluene, this value becomes 4.3%, mostly as a result of the higher density of states.

A second example concerns the barrier found along the reaction path of the dissociation of protonated fluorobenzene [41]. About one-half of the energy of the barrier is released as translation. Similar orders of magnitude were derived by Aschi and coworkers both experimentally [60] and from classical trajectory calculations [61], and by the group of Kim [62,63].

5.7. Nonadiabatic reactions

Up to now, we have focussed on reactions taking place on the ground electronic state of the molecular ion. Interesting effects

are observed when excited electronic states are involved. They can be classified into two categories: (i) the reaction may involve a nonadiabatic transition taking place at a curve crossing along the reaction path; (ii) excited electronic states that are populated by the initial ionization event may, in special situations, decay, possibly partially, to fragments before internal conversion to the ground state takes place. Such a process is usually referred to as an "isolated state decay" and has been mostly observed for fluorine-containing ions. Two examples will be briefly mentioned to illustrate these aspects.

The hydrogen loss fragmentation of the benzene cation at energies where only the lowest asymptote is accessible,

$$C_6H_6{}^+[(\sigma_{CH})^2\pi^5]({}^2B_1 \text{or} {}^2A_2) \rightarrow C_6H_5{}^+[\pi^6]({}^1A_1) + H[1s]({}^2S),$$

is inherently nonadiabatic because of the difference of the electronic configurations of the reactant and of the product states [64].[2] The $^2A_2$ and $^2B_1$ states have been calculated (see footnote 2) to cross the $^2A_1$ state, which correlates with the lowest dissociation asymptote, at a CH distance of about 2.4 Å along the hydrogen loss reaction path. The most surprising and interesting experimental result is that this fragmentation releases more kinetic energy than statistically expected, whereas the opposite is true for the halogenobenzene ($C_6H_5X^+$) C–X fragmentations. This effect is less critical for the perdeuterated isotopomer. It has been shown that the nonadiabatic nature of the reaction is the central argument explaining this behaviour. On one hand, only a small subspace of the vibrational configuration space is involved in the calculation of the nonadiabatic transition probability. This leads in turn to a reduction of the density of active vibrational states and thus to a decreased probability to release energy as vibration. On the other hand, the dissociation rate constant of the $^2A_2$ state has been found to increase as the final orbital angular momentum of the pair of fragments increases, i.e., when their relative kinetic energy grows up, because the curve crossing position moves to shorter CH distances, thus enhancing the probability of the nonadiabatic reaction (see footnote 2).

As a second example, let us consider the fluorine loss reaction of the 1,1-difluoroethene cation ($C_2H_2F_2{}^+$), for which the possibility of a non-statistical mechanism has been suggested already in 1965 by Chava Lifshitz [65] and whose KERD has been recently remeasured and analyzed in detail in the metastable time window (average internal energy ≈0.2 eV above the dissociation threshold) and at higher energies ($\langle E \rangle$ = 1.5–3 eV) [44]. New ab initio calculations have been instrumental in the interpretation of the experimental data. In both energy ranges, the KERD is found to be bimodal and this behaviour has been related to the intervention of excited states in the dissociation mechanism. The first, low-kinetic energy, narrow component is due to a statistical (the ergodicity index is close to 100%) adiabatic dissociation from the ground ionic state of $C_2H_2F_2{}^+$, $\tilde{X}^2B_1$, which correlates with the lowest dissociation asymptote. This state is also diabatically correlated with excited fragments. The second contribution observed in the metastable time range is interpreted as resulting from a diabatic dissociation pathway that crosses repulsive states during the fragment receding motion, finally leading to ground state fragments, but with a larger kinetic energy release. The ergodicity index is then much smaller, about 40%. The broad, bell-shaped, high-kinetic energy contribution recorded in the 1.5–3 eV internal energy range results from a direct dissociation, prior to energy randomization, of excited $\tilde{B}^2A_1$ and $\tilde{C}^2B_2$ states, which are initially populated by the Franck–Condon ionization process and which are repulsive along the C–F reaction coordinate. The fraction of the available phase space explored is very small, in the 10–20% range.

6. Concluding remarks

MEM is very powerful in extracting chemical information from the kinetic energy release distribution of dissociation fragments. The examples discussed here have highlighted (i) how branching ratios between competitive reaction pathways can be inferred; (ii) the influence of exit channel interactions in the presence of a reverse activation barrier; (iii) the role of excited electronic states in certain dissociation mechanisms.

However, an everlasting problem in the dynamics of barrierless reactions concerns the influence of the conservation laws of angular momentum. The study of KERDs provides here also some precious pieces of information. The importance of the contribution provided by the OTST is not to be denied. However, this theory presupposes the validity of equilibrium methods of statistical mechanics in which it introduces a $\{\vec{j}, \vec{\ell}\} \rightarrow \vec{J}$ coupling scheme between angular momenta. Furthermore, it introduces a centrifugal barrier calculated by the simple Langevin theory of ion-induced dipole interactions. These assumptions are not always secure and severely limit the validity of OTST.

A different and complementary strategy is presented here. MEM has no problems with nonequilibrium processes. Simple reactions (in the sense previously defined) are as a rule observed to be characterized by a KERD that obeys Eq. (12) (i.e., where the constraint can be identified with the momentum $\varepsilon^{1/2}$ and where the Lagrange multiplier is positive). Such a situation implies the validity of the RPH model, which has been designed to study reactions with a moderately curved reaction coordinate. Thus, an experimental study of the KERD can be expected to be diagnostic for the validity of a dynamical model directly derived from quantum chemistry. Furthermore, the MEM reveals an unexpected propensity to reduce the dimensionality of the translational motion of the fragments to a two-dimensional space, even when OTST is no longer valid. The relationship between this propensity and angular momentum conservation is straightforward when the interaction potential is isotropic. However, for hitherto unknown reasons, it apparently subsists in more complicated cases. It is also clear that at high internal energy, the most critical feature of a barrierless reaction is the curvature of the reaction coordinate.

It would have been enlightening to discuss all this with Chava. Her experimental skill, her perceptive advice, her

[2] E. Gridelet, R. Locht, A.J. Lorquet, J.C. Lorquet, B. Leyh, J. Phys. Chem. A (2006), submitted for publication.

tremendous culture resulting from a wide variety of interests are sorely missed.

Acknowledgments

We are grateful to our colleagues, coworkers and former graduate students whose contributions to the results presented in this short review have been instrumental: Dr. F. Remacle, Dr. A.J. Lorquet, Dr. D. Dehareng, Dr. P. Urbain, Dr. A. Hoxha, and Dr. D. Fati. Financial support from the Belgian F.N.R.S. and from the Gouvernement de la Communauté Française de Belgique (Action de Recherche Concertée, ARC 99-04/245) is gratefully acknowledged.

References

[1] T. Baer, W.L. Hase, Unimolecular Reaction Dynamics. Theory and Experiments, Oxford University Press, New York, 1996.
[2] R.G. Gilbert, S.C. Smith, Theory of Unimolecular and Recombination Reactions, Blackwell Scientific Publications, Oxford, UK, 1990.
[3] W. Forst, Unimolecular reactions, in: A Concise Introduction, Cambridge University Press, Cambridge, 2003.
[4] H.M. Rosenstock, M. Krauss, Adv. Mass Spectrom. 2 (1963) 251.
[5] F. Remacle, R.D. Levine, J. Phys. Chem. 95 (1991) 7124.
[6] C. Lifshitz, Adv. Mass Spectrom. 7A (1978) 3.
[7] C. Lifshitz, Int. J. Mass Spectrom. Ion Phys. 43 (1982) 179.
[8] C. Lifshitz, J. Phys. Chem. 87 (1983) 2304.
[9] C. Lifshitz, Adv. Mass Spectrom. 12 (1992) 315.
[10] J. Laskin, C. Lifshitz, J. Mass Spectrom. 36 (2001) 459.
[11] T. Baer, Adv. Chem. Phys. 64 (1986) 111.
[12] I. Powis, Acc. Chem. Res. 20 (1987) 179.
[13] C.E. Klots, J. Phys. Chem. 75 (1971) 1526.
[14] C.E. Klots, Z. Naturforsch. 27a (1972) 553.
[15] W.J. Chesnavich, M.T. Bowers, J. Am. Chem. Soc. 98 (1976) 8301.
[16] W.J. Chesnavich, M.T. Bowers, J. Am. Chem. Soc. 99 (1977) 1705.
[17] W.J. Chesnavich, M.T. Bowers, J. Chem. Phys. 66 (1977) 2306.
[18] W.J. Chesnavich, M.T. Bowers, in: M.T. Bowers (Ed.), Gas-Phase Ion Chemistry, Academic Press, New York, 1979.
[19] W.J. Chesnavich, M.T. Bowers, Prog. React. Kinet. 11 (1982) 137.
[20] E.E. Nikitin, Theory of Elementary Atomic and Molecular Processes in Gases, Clarendon Press, Oxford, 1974.
[21] B. Leyh, J.C. Lorquet, in: P.B. Armentrout (Ed.), The Encyclopedia of Mass Spectrometry, Elsevier, Amsterdam, 2003, p. 17.
[22] E. Gridelet, J.C. Lorquet, B. Leyh, J. Chem. Phys. 122 (2005) 094106.
[23] L. Bonnet, P. Larrégaray, J.-C. Rayez, Phys. Chem. Chem. Phys. 7 (2005) 3540.
[24] W.H. Miller, N.C. Handy, J.E. Adams, J. Chem. Phys. 72 (1980) 99.
[25] W.H. Miller, J. Phys. Chem. 87 (1983) 3811.
[26] S.H. Lim, J.C. Choe, M.S. Kim, J. Phys. Chem. A 102 (1998) 7375.
[27] R.D. Levine, R.B. Bernstein, in: W.H. Miller (Ed.), Dynamics of Molecular Collisions Part B, Plenum Press, New York, 1976.
[28] Y. Alhassid, R.D. Levine, J. Chem. Phys. 67 (1977) 4321.
[29] R.D. Levine, J.L. Kinsey, in: R.B. Bernstein (Ed.), Atom–Molecule Collision Theory. A Guide for the Experimentalist, Plenum, New York, 1979.
[30] R.D. Levine, Adv. Chem. Phys. 47 (1981) 239.
[31] R.D. Levine, in: M. Baer (Ed.), Theory of Chemical Reaction Dynamics, CRC Press, Boca Raton, Fl, 1985.
[32] W. Forst, Theory of Unimolecular Reactions, Academic Press, New York, 1973 (footnote 10, p. 55).
[33] D.M. Leitner, P.G. Wolynes, Chem. Phys. Lett. 258 (1996) 18.
[34] D.M. Leitner, P.G. Wolynes, Chem. Phys. Lett. 280 (1997) 411.
[35] R.D. Levine, Ber. Bunsenges. Phys. Chem. 78 (1974) 111.
[36] J.C. Lorquet, Mass Spectrom. Rev. 13 (1994) 233.
[37] P. Urbain, F. Remacle, B. Leyh, J.C. Lorquet, J. Phys. Chem. 100 (1996) 8003.
[38] P. Urbain, B. Leyh, F. Remacle, A.J. Lorquet, R. Flammang, J.C. Lorquet, J. Chem. Phys. 110 (1999) 2911.
[39] P. Urbain, B. Leyh, F. Remacle, J.C. Lorquet, Int. J. Mass Spectrom. 185/186/187 (1999) 155.
[40] A. Hoxha, R. Locht, A.J. Lorquet, J.C. Lorquet, B. Leyh, J. Chem. Phys. 111 (1999) 9259.
[41] J.C. Lorquet, A.J. Lorquet, J. Phys. Chem. A 105 (2001) 3719.
[42] E. Gridelet, R. Locht, A.J. Lorquet, J.C. Lorquet, B. Leyh, Int. J. Mass Spectrom. 228 (2003) 389.
[43] D. Fati, A.J. Lorquet, R. Locht, J.C. Lorquet, B. Leyh, J. Phys. Chem. A 108 (2004) 9777.
[44] E. Gridelet, D. Dehareng, R. Locht, A.J. Lorquet, J.C. Lorquet, B. Leyh, J. Phys. Chem. A 109 (2005) 8225.
[45] F. Iachello, R.D. Levine, Europhys. Lett. 4 (1987) 389.
[46] R.D. Levine, Adv. Chem. Phys. 70 (1988) 53.
[47] T. Baer, J. Booze, K.M. Weitzel, in: C.Y. Ng (Ed.), Vacuum Ultraviolet Photoionization and Photodissociation of Molecules and Clusters, World Scientific, Singapore, 1991, p. 259.
[48] J.C. Lorquet, J. Phys. Chem. A 104 (2000) 5422.
[49] Y. Malinovich, R. Arakawa, G. Haase, C. Lifshitz, J. Phys. Chem. 89 (1985) 2253.
[50] Y. Malinovich, C. Lifshitz, J. Phys. Chem. 90 (1986) 2200.
[51] C. Lifshitz, F. Louage, V. Aviyente, K. Song, J. Phys. Chem. 95 (1991) 9298.
[52] M.A. Collins, Adv. Chem. Phys. 93 (1996) 389.
[53] V.B. Pavlov-Verevkin, J.C. Lorquet, J. Chem. Phys. 123 (2005) 074324.
[54] M.A. Haney, J.L. Franklin, J. Chem. Phys. 48 (1968) 4093.
[55] J.C. Lorquet, Int. J. Mass Spectrom. 200 (2000) 43.
[56] J.C. Lorquet, B. Leyh, in: P.B. Armentrout (Ed.), The Encyclopedia of Mass Spectrometry, Elsevier, Amsterdam, 2003, p. 33.
[57] C. Lifshitz, Acc. Chem. Res. 27 (1994) 138.
[58] J.H. Moon, J.C. Choe, M.S. Kim, J. Phys. Chem. A 104 (2000) 458.
[59] D. Schröder, I. Oref, J. Hrusak, T. Weiske, E.E. Nikitin, W. Zummack, H. Schwarz, J. Phys. Chem. A 103 (1999) 4609.
[60] M. Aschi, F. Grandinetti, F. Pepi, Int. J. Mass Spectrom. Ion Process. 130 (1994) 117.
[61] M. Aschi, F. Grandinetti, Eur. J. Mass Spectrom. 6 (2000) 31.
[62] T.G. Lee, M.S. Kim, S.C. Park, J. Chem. Phys. 104 (1996) 5472.
[63] T.H. Choi, S.T. Park, M.S. Kim, J. Chem. Phys. 114 (2001) 6051.
[64] S.J. Klippenstein, Int. J. Mass Spectrom. Ion Process. 167/168 (1997) 235.
[65] C. Lifshitz, F. Long, J. Phys. Chem. 69 (1965) 3737.